scientific reports

Check for updates

OPEN

Enhancing radiation-induced reactive oxygen species generation through mitochondrial transplantation in human glioblastoma

Kent L. Marshall[1], Murugesan Velayutham[2], Valery V. Khramtsov[2], Alan Mizener[3] & Christopher P. Cifarelli[1,3,4]✉

Glioblastoma (GBM) is the most aggressive primary brain malignancy in adults, with high recurrence rates and resistance to standard therapies. This study explores mitochondrial transplantation as a novel method to enhance the radiobiological effect (RBE) of ionizing radiation (IR) by increasing mitochondrial density in GBM cells, potentially boosting reactive oxygen species (ROS) production and promoting radiation-induced cell death. Using cell-penetrating peptides (CPPs), mitochondria were transplanted into GBM cell lines U3035 and U3046. Transplanted mitochondria were successfully incorporated into recipient cells, increasing mitochondrial density significantly. Mitochondrial chimeric cells demonstrated enhanced ROS generation post-irradiation, as evidenced by increased electron paramagnetic resonance (EPR) signal intensity and fluorescent ROS assays. The transplanted mitochondria retained functionality and viability for up to 14 days, with mitochondrial DNA (mtDNA) sequencing confirming high transfection and retention rates. Notably, mitochondrial transplantation was feasible in radiation-resistant GBM cells, suggesting potential clinical applicability. These findings support mitochondrial transplantation as a promising strategy to overcome therapeutic resistance in GBM by amplifying ROS-mediated cytotoxicity, warranting further investigation into its efficacy and mechanisms in vivo.

Keywords Glioblastoma, Mitochondria, ROS, EPR, Radiation, Cell-penetrating peptide, RBE

Glioblastoma remains the most common, aggressive, and lethal primary brain malignancy in adults despite incremental advances in management over the past three decades[1,2]. While the standard of care (SOC) for management of GBM typically includes maximal safe surgical resection followed by chemoradiotherapy, disease progression is invariable. In fact, the 2-year local recurrence rate of GBM is estimated to be 90% despite multimodal therapy with remaining malignant cells often progressing with phenotypes which are more resistant to pharmacological intervention and radiotherapy[3–5]. Further complicating the issue, there are currently no consensuses on the SOC for recurrent GBM making the establishment of new options for therapy for the management of both primary and recurrent GBM paramount for improving patient survival and quality of life.

Radiation treatment has played a pivotal role in the treatment of GBM for decades and represents one the few therapies where Level 1 clinical evidence supports use. As with other malignancies, the DNA damage incurred after exposure to ionizing radiation (IR) impacts rapidly dividing GBM cells and leads to local toxic effects in the presence of impaired DNA damage response (DDR) mechanisms[6]. Central to this cytotoxic process is the intracellular production of reactive oxygen species (ROS), primarily by the radiolysis of water and the generation of hydroxyl radicals (OH·), with downstream generation of other radical species, such as superoxide anions (O_2·) and hydrogen peroxide (H_2O_2). In total, all ROS can damage macromolecular structures like lipids, proteins, and DNA[7,8]. Under normal physiological circumstances, the mitochondria are the primary source of intracellular ROS, designated mtROS[9,10]. IR can induce OH· through radiolysis of water within the mitochondria; however

[1]Department of Neurosurgery, Rockefeller Neuroscience Institute, West Virginia University, 1 Medical Center Drive, Morgantown, WV 26506-9183, USA. [2]Department of Biochemistry and Molecular Medicine, West Virginia University, Morgantown, WV, USA. [3]West Virginia University Cancer Institute, Morgantown, WV, USA. [4]Department of Radiation Oncology, West Virginia University, Morgantown, WV, USA. ✉email: cpcifarelli@hsc.wvu.edu

it can also alter the structure and function of mitochondria leading to breakdown of the electron transport chain (ETC) and oxidative phosphorylation leading to sustained production of ROS[11,12]. These damaged mitochondria contribute to apoptotic responses directly through expulsion of pro-apoptotic signaling molecules like cytochrome C and caspases[13].

While radiation improves the survival and quality of life in GBM patients, recurrence and associated radiation resistant phenotypes lead to eventual therapeutic failure. There have been recent attempts, to develop novel compounds or repurpose existing pharmaceuticals to sensitize or re-sensitize GBM to radiotherapy including temozolomide, quisinostat, difluorodeoxyuridine, among others[14,15]. However, these compounds have only demonstrated modest improvement in radiotherapy for GBM and guidelines currently do not support the use of radiosensitizers in CNS disease[16,17]. Moving beyond direct pharmaceutical-based interventions, precision medicine efforts could be focused on improving the radiobiological effect (RBE) of IR through increasing the density of mitochondria within a population of tumors cells targeted for radiation-induced cell death.

Mitochondrial transplantation has been described in context of deficiency diseases such as, myoclonic epilepsy with ragged red fibers (MERRF), mitochondrial encephalomyopathy with lactic acidosis and stroke-like episodes (MELAS), and Leber hereditary optic neuropathy (LHON)[18,19]. Regardless of the success, or lack thereof, in these models, the current literature supports the successful incorporation of exogenous mitochondria into donor cells using cell-penetrating peptides (CPPs)[20]. Increasing the number of mitochondria in neoplastic cells will potentially allow for the generation of more ROS and pro-apoptotic molecules and lead to an improved response to radiation and radiobiological effect. Therefore, this study aims to provide proof-of-concept for the transfer of exogenous mitochondria into GBM cell lines in order to evaluate the feasibility, efficacy, and durability of mitochondrial transplantation as a precision medicine tool for radiotherapy.

Results

Exogenous allogenic and autologous transplant is possible between distinct GBM cell lines

Mitochondria extracted from donor U3035 cells were successfully incorporated into the cytoplasm of recipient U3035 cells at concentrations of 100 µg and 300 µg of mitochondrial protein/5.0 $\times$ 10^5 U3035 cells. (Fig. 1B–G). Quantification of mitochondria labelling intensity between native U3035 cells and 1X and 3X autologous mitochondria transplants revealed statistically significant differences ($p < 0.001$; Fig. 1A). Western blotting for cytochrome C confirmed the presence of relatively more mitochondrial associated protein in the 1X and 3X autologous transplants compared to the native U3035 cells (Fig. 1H).

Mitochondria extracted from donor U3020 cells were also successfully incorporated into the cytoplasm of recipient U3035 cells at a concentration of 100 µg of mitochondrial protein/5.0 $\times$ 10^5 U3035 cells and signals persisted through post-transplant day 7 (Fig. 2A–E) generating allogenic U3035Mt20-chimeras. Scatter plot analysis of MITO Red (donor mitochondrial) versus MITO Green (native mitochondria) confirmed a positive correlation with a mean intensity increase of 1.3-fold in donor mitochondria to native mitochondria (1.038×10^4 vs. 7849 RFU, respectively) (Fig. 2F). Additional cell lines were used in a similar manner, with U3035 donor mitochondria transplanted into U3046 recipient cells (Fig. 2G–J). Once again, scatter plot demonstrated a positive correlation with mean intensity increase of 3.1-fold in donor mitochondria to native mitochondria (1.561×10^4 vs. 5106 RFU, respectively).

Mitochondrial density was distinct between individual GBM lines and chimeras

Mitochondrial densities were determined using total nanograms of mitochondrial protein per cell following mitochondrial isolation procedures. U3035 cells had a baseline mean mitochondrial density of 0.135 ± 0.04 ng/cell while U3020 cells had a baseline mean density of 0.28 ± 0.1 ng/cell (Fig. 3). Following allogenic transplant, U3035Mt20-1X chimeras had a density of 0.38 ± 0.1 ng/cell 7 days post-transplant, which represented a significant increase over the baseline U3035 donor measurement ($p = 0.003$). Furthermore, the U3035Mt20-3X chimeras demonstrated a mitochondrial density of 0.76 ± 0.07 ng/cell 7 days post-transplant, which represents a significant increase in density when compared to both the U3035 donor cells ($p < 0.0001$) and U3035Mt20-1X chimeras ($p < 0.0001$). In order to demonstrate the dynamic nature of the mitochondrial density within GBM cells, U3020 and U3035 cells were cultured under hypoxic conditions. U3020 and U3035 hypoxic cells had mitochondrial densities of 0.121 ± 0.025 and 0.063 ± 0.04 ng/cell respectively.

Mitochondrial Chimeric cells increased the amount of reactive oxygen species generated following exposure to ionizing radiation

When exposed to 8 Gy of low-energy X-ray radiation (220 kV), U3020 cells and U3035 cells exhibited similar generation of hydroxyl radicals as measured by absolute signal intensity of EPR (0.248 ± 0.006 and 0.246 ± 0.007, respectively) (Fig. 4). U3035Mt20-1X chimeras showed a significant increase in EPR signal intensity (0.311 ± 0.01) as compared to the U3035 cells alone ($p = 0.02$). U3035Mt20-3X chimeras showed a significantly higher EPR signal intensity at 0.453 ± 0.03 as compared to both U3035 cells and U3035Mt20-1X chimeras ($p < 0.0001$ for both comparisons). There were no appreciable differences between allogenic and autologous chimeric cell lines. These data were confirmed using a fluorescent pan-ROS assay (Fig. 5). U3035Mt20-3X chimeras showed a marked increase in overall ROS following 8 Gy irradiation at 0.5 and 24 h vs their 0 Gy baseline as compared to radiation responses in the native U3035 cells. U3035Mt20-3X chimeras exhibited a fluorescent signal intensity 2.3-fold higher at 0.5 h and 3.3-fold higher at 24 h. Change in ROS signal intensity was greater in U3035Mt20-3X chimeras when compared to U3035 ($p = 0.005$) but not U3020 ($p = 0.14$) at 0.5 h post-irradiation. U3035 and U3020 cells showed a response similar to one another following 8 Gy irradiation at 0.5 h with 1.7- and 1.2- fold increases, respectively ($p = 0.26$). When 24 h signals were compared for 8 Gy, there were significant differences observed between the GBM lines. U3020 had a sustained increase in ROS level (1.9-fold increase) while U3035

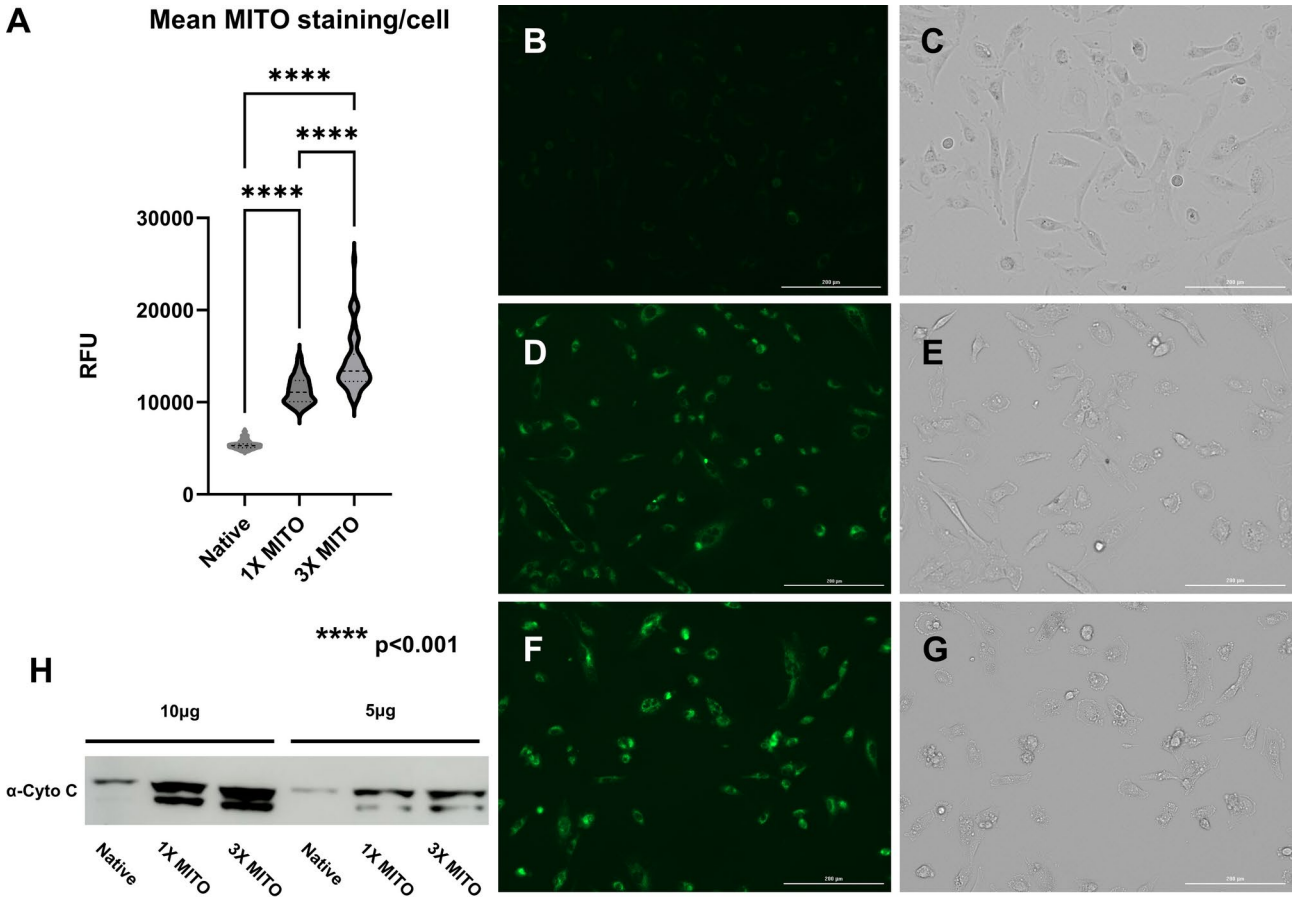

Fig. 1. Use of cell-penetrating peptides (CPPs) to increase mitochondria fraction in human U3035 GBM cells. Representative images of native U3035 cells (**B**,**C**) were compared to U3035 cells receiving 100 µg of isolated and MITO Green labelled mitochondria (1X; **D**,**E**) and 300 µg of isolated and MITO Green labelled mitochondria (3X; **F**,**G**). 10X magnification with 200 µm scale bar shown. ANOVA of mean intensities per cell analyzed (native n = 67; 1X n = 79; 3X n = 57) demonstrated statistical significance in differences across all groups ($p < 0.001$). Western blotting for cytochrome C in native U3035 cells and 1X and 3X U3035 mitochondrial transplants confirmed the increase in the mitochondrial protein in the transplants relative to the native cells (**H**). Original blot is presented in Supplementary Fig. S1.

did not (1.2-fold increase). The 3.3-fold increase in the 24 h ROS signal observed in the U3035Mt20-3X chimeras was significantly greater than those observed in both U3020 and U3035 ($p < 0.001$ for both).

Mitochondrial transplants were durable

Analysis of mitochondrial DNA (mtDNA) sequencing from the 14-day U3035Mt20-3X chimera revealed a total of 37 heteroplasmic positions. 32 of these heteroplasmic positions were concordant with either 3020 donor or 3035 recipient sequences (Fig. 6, *gray*). The average allele frequency for 3020 donor sequences was 91.9%, while the average allele frequency for 3035 recipient sequences was 8.1%. The high degree of similarity with donor mitochondrial sequences suggests a high mitochondrial transfection and retention rate 14 days post-transfection. The remaining 5 heteroplasmic positions had de novo sequences that were not detected in either of the original cell lines (Fig. 6, *orange*). All de novo sequences had allele frequencies below 4%. A further 7 single nucleotide polymorphisms (SNPs) detected when comparing the non-chimeric 3020 donor and 3035 recipient mitochondrial sequences were completely converted (allele frequency > 99%) to 3020 donor sequences in the chimeric cell line (Fig. 6, *blue*).

Mitochondrial transplant was possible in cells with an induced radio-resistant phenotype

U3035 cells were treated with 6 fractions of 2 Gy Xray radiation for a total radiation dose of 12 Gy to demonstrate a cell line with prior radiation exposure. Following generation of the radioresistant U3035 line, 1X allogenic mitochondrial transplants were established and persisted to post-transplant day 7 (Fig. 7A–E). Cells proliferated and survived past post-transplant day 10 with a subsequent loss vital dye signal. Scatter plot analysis of MITO Red (donor mitochondrial) versus MITO Green (native mitochondria) confirmed a positive correlation with a mean intensity increase of 1.8-fold in donor mitochondria to native mitochondria (1.497×10^4 vs. 7983 RFU, respectively) (Fig. 7F).

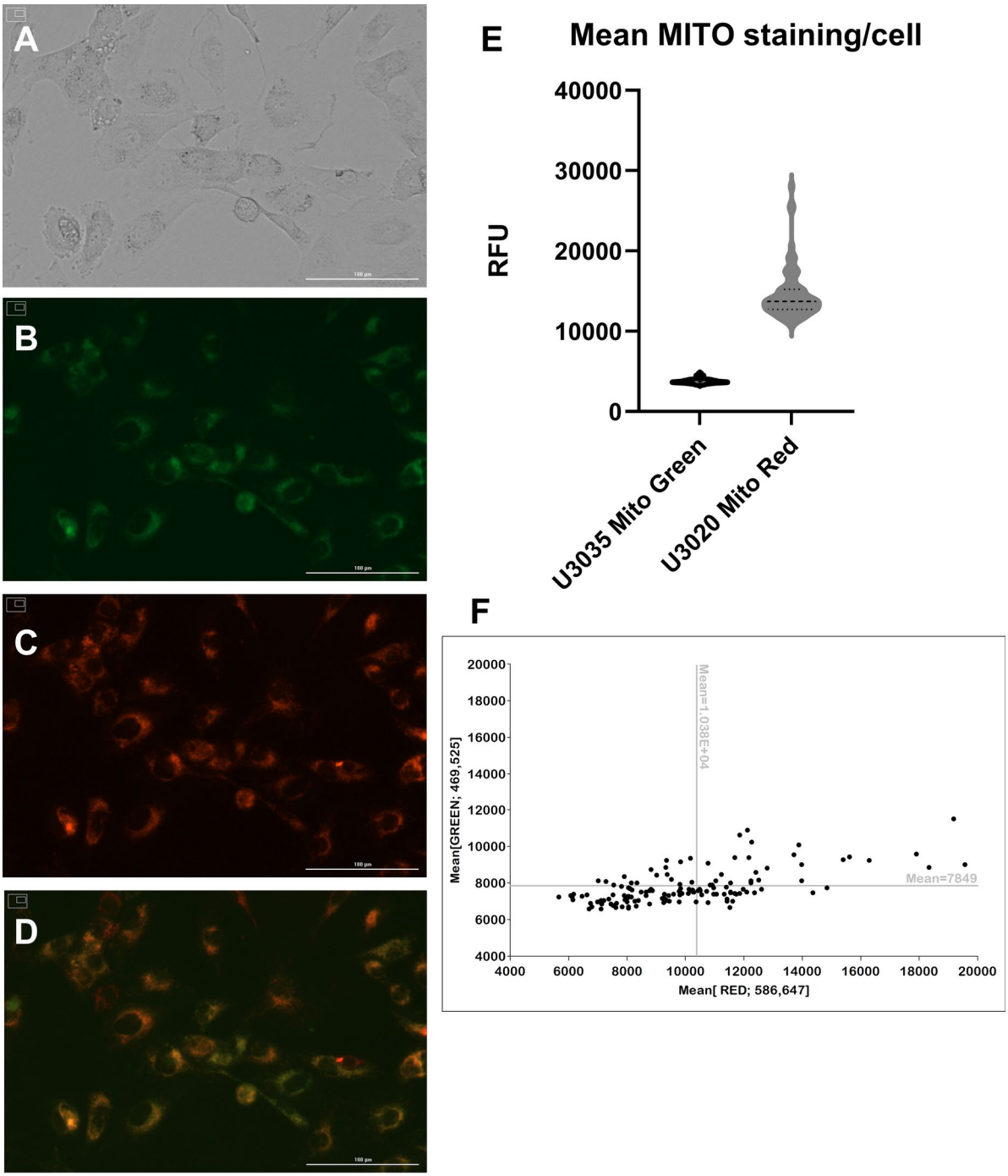

Fig. 2. Proof of concept for allogenic mitochondrial transplantation in human GBM cell lines. Using donor mitochondria from multiple human GBM cells lines (U3020 and U3035; MITO Red), CPPs were used to transplant 100 µg of mitochondria into recipient cells (U3035 (**A**–**E**) and U3046 (**G**–**K**); MITO Green). Scatter plots of mean staining intensities of native vs. donor mitochondria are presented in panel (**F**) (U3035-U3020; n = 77) and panel (**L**) (U3046-3035; n = 139) with a 1.3-fold and threefold increase in donor vs recipient mitochondrial fluorescence intensity in the U3035-U3020 and U3046-U3035 chimera, respectively. All images were acquired at 60X with 100 µm scale bars noted.

Discussion

Our understanding of the role of metabolic pathways in the tumorigenesis and development of treatment resistance in glioblastoma (GBM) continues to expand. The importance of isocitrate dehydrogenase (IDH) isotype mutants in the latest WHO classification system underscores the fundamental importance of tumor cell metabolism in prognostication, while IDH-based therapy offers therapeutic promise in IDH-mutant tumors[21,22]. Although the majority of clinical interest has been placed on determining mutation/epigenetic status in

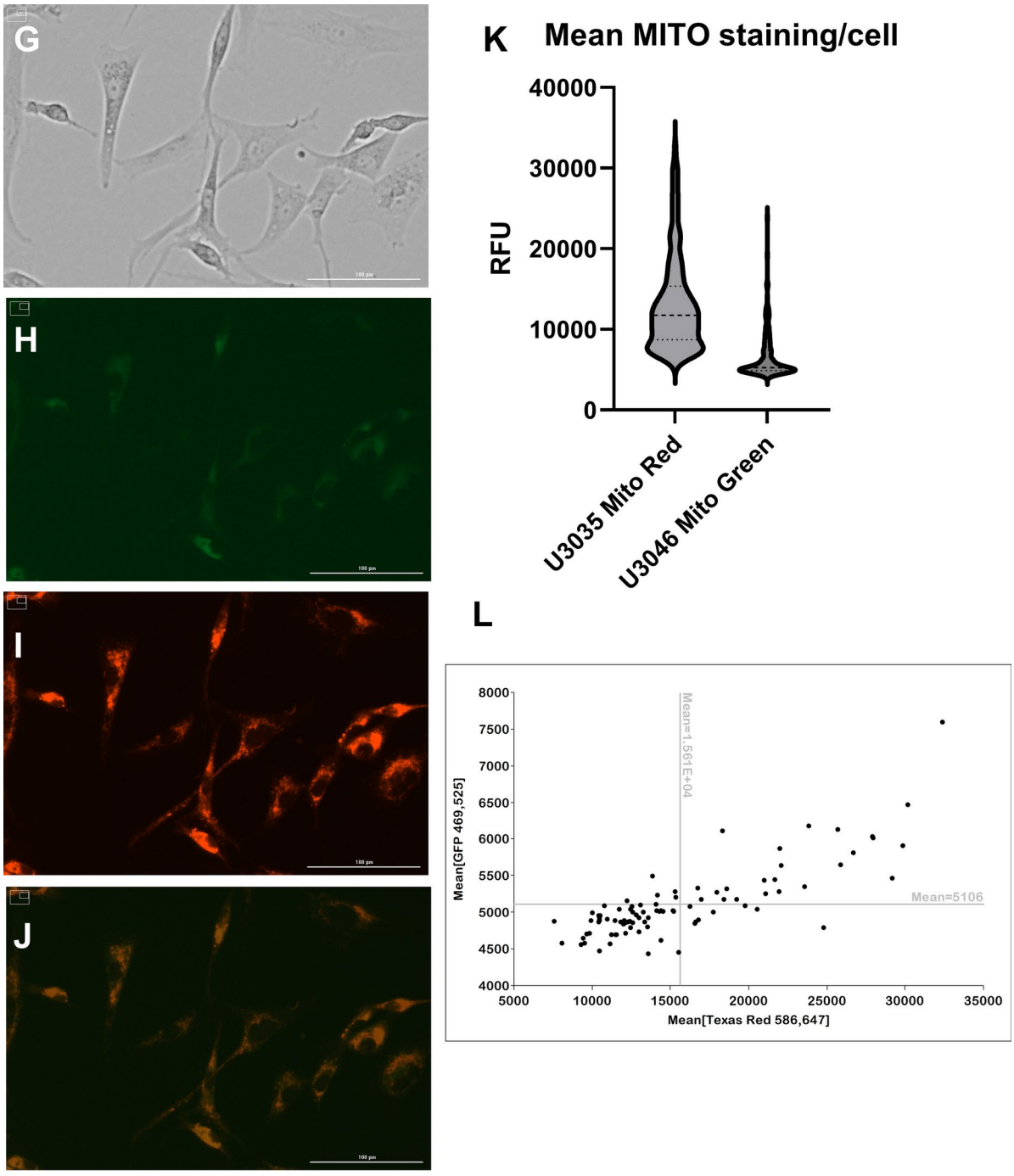

Figure 2. (continued)

diagnostic patient specimens, a wealth of preclinical data have emerged regarding the role that mitochondria play and their potential to form relevant reactive oxygen species (ROS). For example, the increased action of mitochondrial superoxide dismutase 2 (SOD2) in glioblastoma has been attributed with a role in the development of resistance to temozolomide, the first-line standard of care chemotherapeutic[23,24]. Similarly, evidence supports the upregulation and stabilization of free radical scavenger systems within glioma stem-like cells (GSCs), thereby limiting the accumulation of mitochondrial ROS and conferring radiation resistance[25]. Based on the data in the current study, we propose a methodology for using exogenous donor mitochondria as a means by which to increase mitochondria reactive oxygen species (mtROS) in GBM cells in vitro in response to ionizing radiation exposure.

While the concept of mitochondrial transfer or transplantation is not new, the application of such a process to sensitize a tumor cell to standard therapy, such as radiation, is novel in the context of glioblastoma. Spontaneous mitochondrial transfer has been documented in the CNS, through which non-tumor astrocytic mitochondria

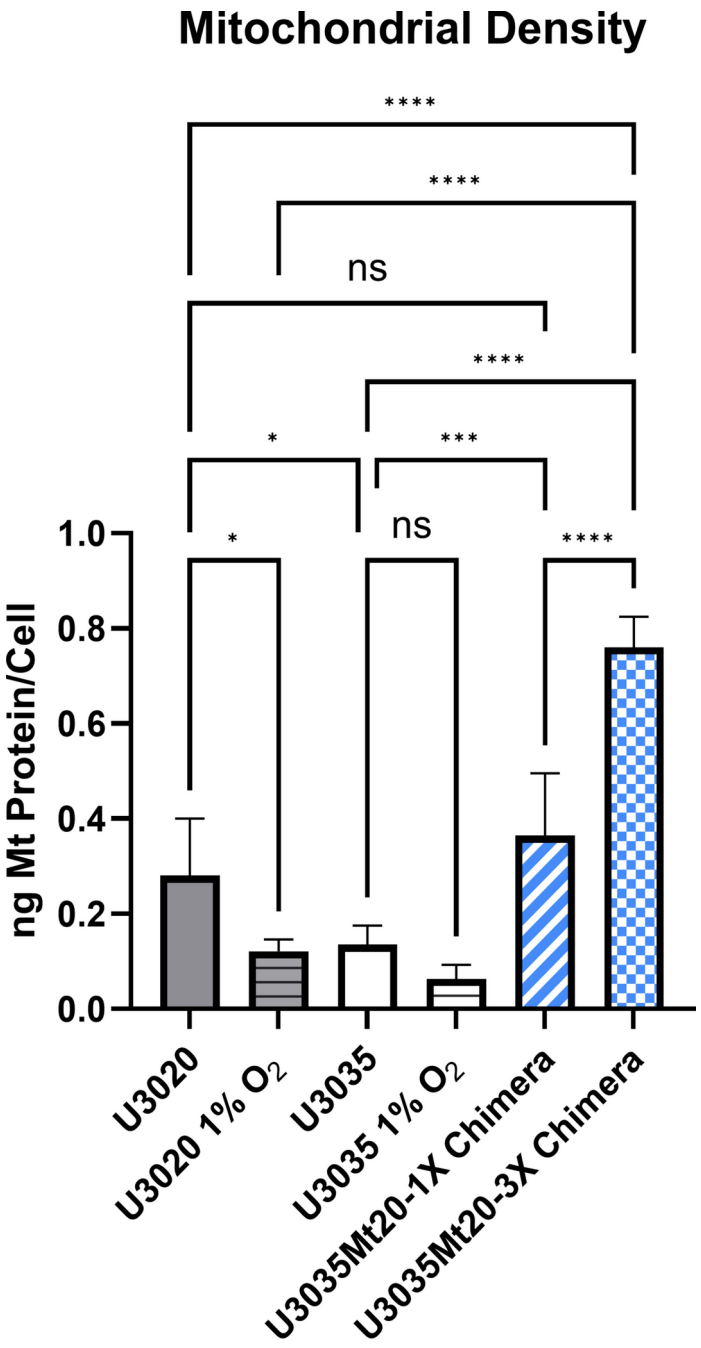

Fig. 3. Quantification of mitochondrial density. Mitochondrial densities from each cell line were obtained by dividing the total mass of mitochondrial protein (ug) that were extracted from individual lines by the number of live cells following dissociation and mitochondrial isolation. To demonstrate the predictable dynamic nature of mitochondrial density, and intact mitochondrial signaling response in the U3020 and U3035 lines, mitochondrial densities were also included from cells cultured under hypoxic conditions. One-way ANOVA was conducted using a Tukey's multiple comparisons pos-hoc test to determine significance in the difference of means between groups. All data were analyzed using * $p < 0.05$ and ** $p < 0.01$.

transferred to GBM cells within the tumor microenvironment[26]. The presence of tunneling nanotubes (TNTs) has been demonstrated in GBM resection specimens while mitochondrial transfer has been demonstrated in vitro between GBM cells and adjacent non-neoplastic astrocytes, conferring resistance to hypoxia and increased glucose- and glutamine-dependence[27]. In the current study, we enlisted the aid of the cell-penetrating peptide (PEP-1; sequence KETWWETWWTEWSQP-KKKRKV) as a means of artificially introducing both allogeneic and autogenic mitochondria into the U3035 and U3046 GBM cell lines. First described in the context of the Tat protein in the human immunodeficiency virus (HIV-1) in 1998 independently by Frankel & Cabo and Green & Loewenstein, cell-penetrating peptides have the potential to deliver significant payloads to the intracellular space

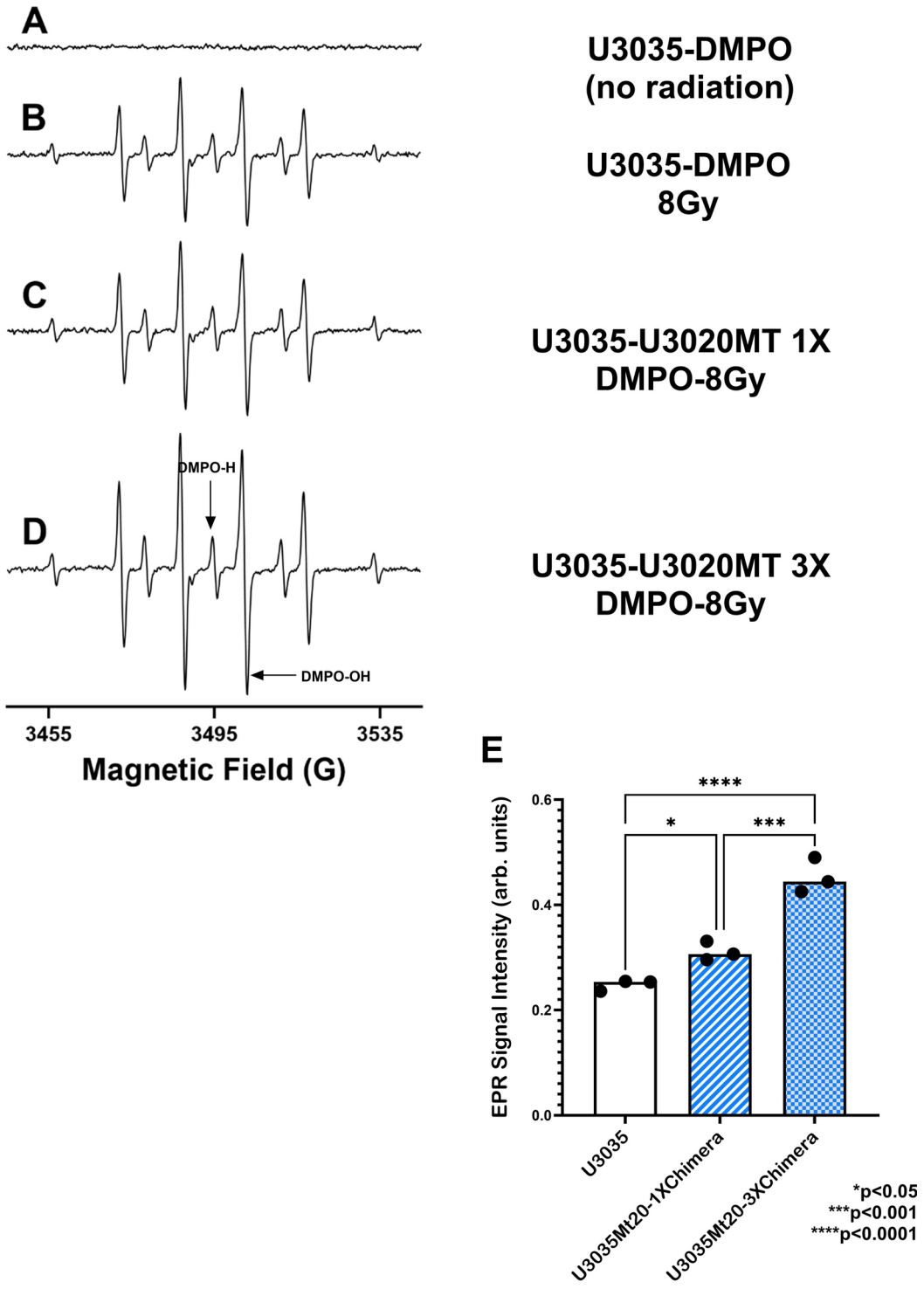

Fig. 4. EPR spectra of DMPO adducts. (**A**) U3035 cells + DMPO (200 mM). (**B**) U3035 cells + DMPO (200 mM) radiated using 8 Gy X-ray. (**C**) U3035 cells transplanted with mitochondria (1X) + DMPO (200 mM) and radiated using 8 Gy X-ray. (**D**) U3035 cells transplanted with mitochondria (3X) + DMPO (200 mM) and radiated using 8 Gy X-ray. (**E**) Quantification of absolute EPR signal intensity among U3035, U3035Mt-1XChimera, and U3035mt-3XChimera (n = 3 each group; *$p < 0.05$; ***$p < 0.001$; ****$p < 0.0001$).

via direct translocation or endocytosis[28]. Within the context of glioblastoma treatment, the use of CPPs has been attempted to facilitate the transfer of chemotherapeutics and immune effectors across the blood brain barrier (BBB) and the brain tumor interface[29,30]. Taking advantage of the CPP technique and using mitochondria from multiple cells lines into recipient human GBM cells, we were successful in confirming that relative mitochondrial content correlates to an increase in ROS, detectable via EPR spin-trapping techniques and mitochondrial dye

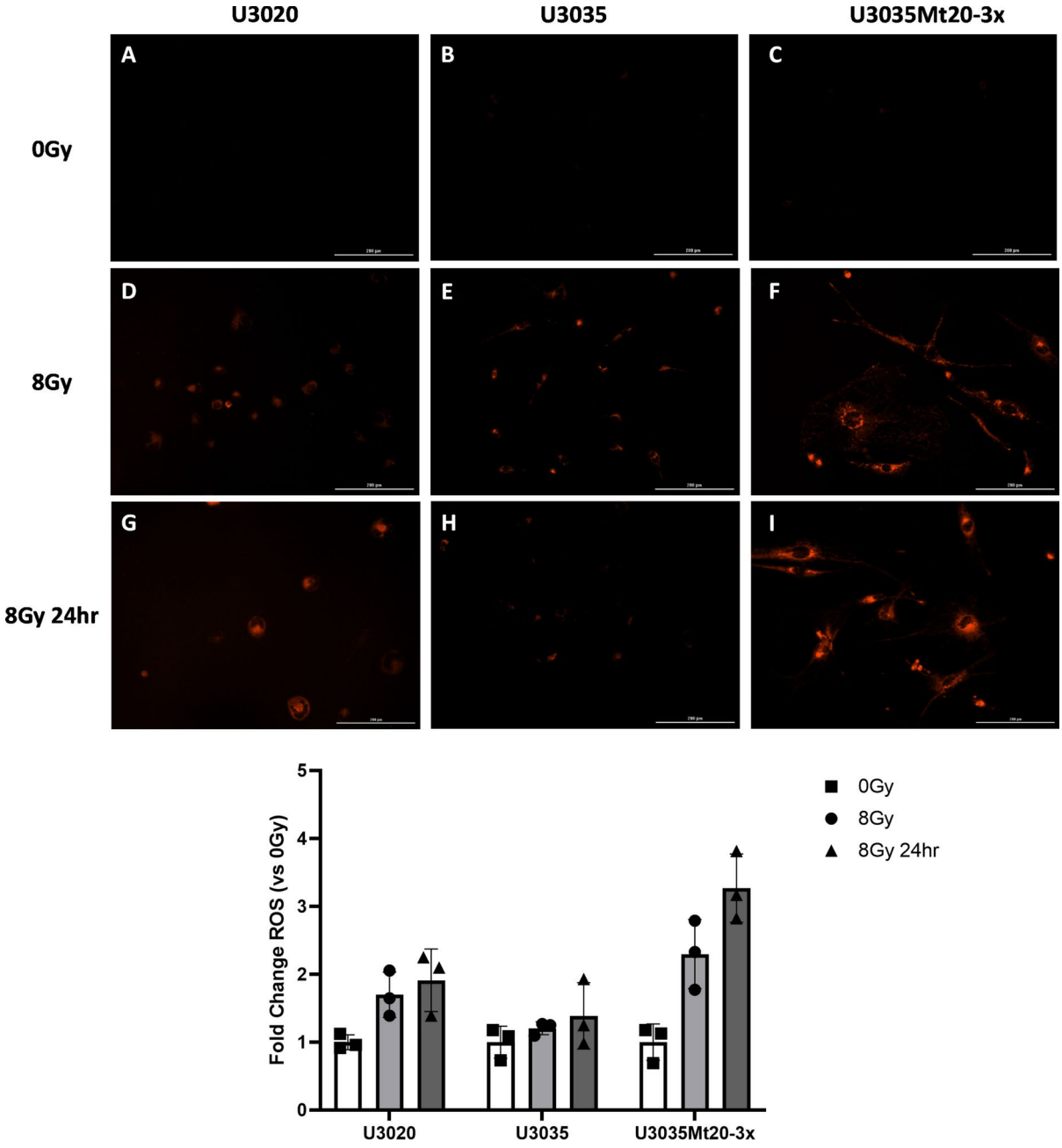

Fig. 5. Fluorescent probe of ROS generation. Representative Images of: U3020, U3035, and U3035Mt20-3 × cells stained with CellROX™ Deep Red fluorescent ROS probe following 0 Gy X-ray irradiation (**A**–**C**). U3020, U3035, and U3035Mt20-3X cells stained with CellROX™ Deep Red fluorescent ROS probe following 8 Gy X-ray irradiation and assayed 1 h following treatment (**D**–**F**). U3020, U3035, and U3035Mt20-3X cells stained with CellROX™ Deep Red fluorescent ROS probe following 8 Gy X-ray irradiation and assayed 24 h following treatment (**D**–**F**). (**G**) Quantification of these data represented by mean fold-change of relative fluorescent units vs 0 Gy as a control.

tracking. These findings are concordant with those in other cell types, namely skeletal muscle[31] and expanded on our previous work in which U3035 cells and U3020 cells displayed differences in ROS longevity, with ROS persisting longer in the more radiation sensitive U3020 cells compared to the relatively resistant U3035 cells[32].

The sustainability of donor mitochondria post-transplantation was also of interest in developing a methodology that would eventually have a practical therapeutic potential use. Whereas the native U3035 GBM cells demonstrated a rapid decay of ROS both in EPR and mitochondrial staining assays, the U3020 GBM cells maintained mitochondrial ROX-staining for at least 24 h post-radiation. With ROS longevity typically limited to milliseconds, thus requiring spin-trapping solvents to confirm their presence, to maintain a durable ROS signal via mitochondrial staining is a promising finding. The durability of the transplantation was also confirmed using

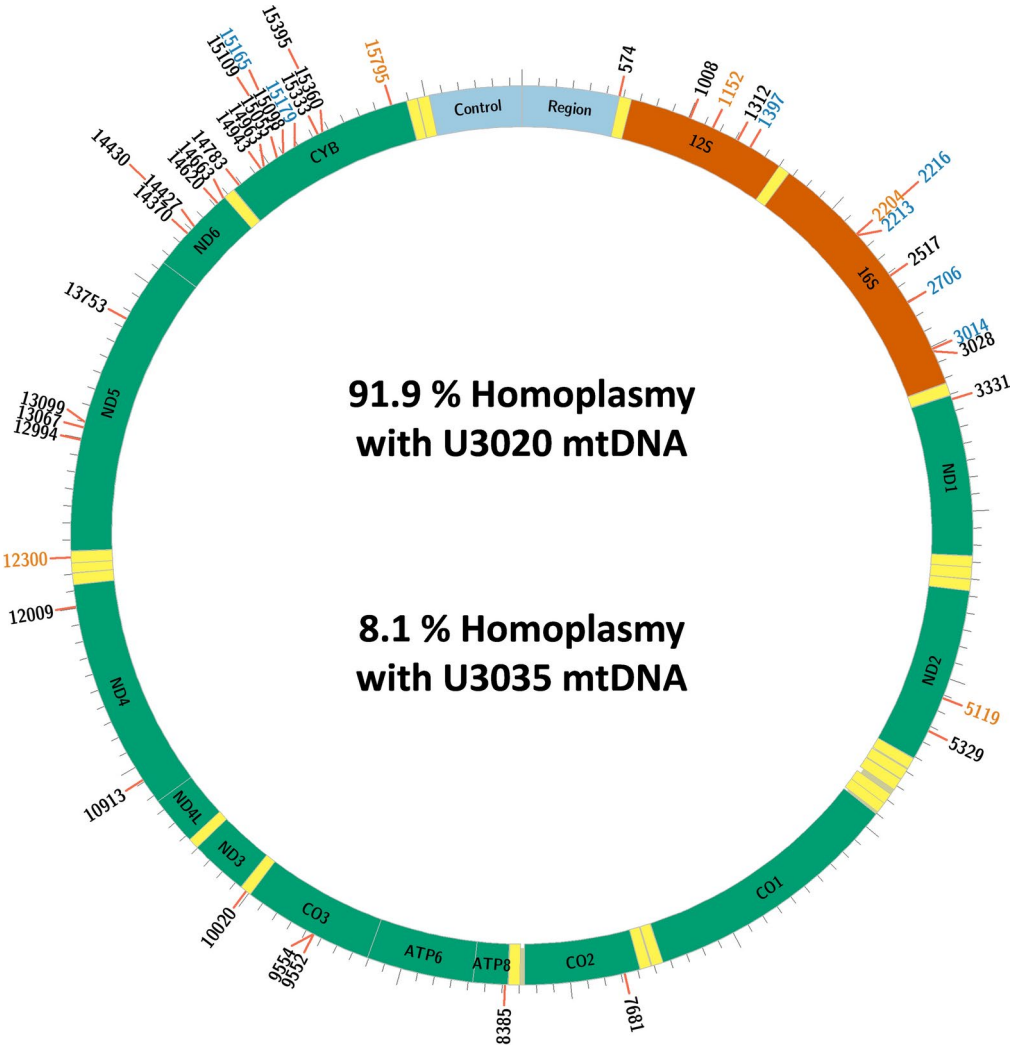

Fig. 6. Mitochondrial DNA sequence analysis within U3035MT20-3 × chimeras following transplantation. A Circos plot designating the circular mitochondrial DNA of the U3035Mt20-X3 chimeras and the single nucleotide polymorphisms that were either shared variably with U3020 or U3035 mtDNA sequences (grey), completely converted to U3020 (blue), or not expressed in either the donor or recipient lines (orange). Allele frequencies were averaged for the grey SNP's and combined with the blue SNPs and it was found that the DNA sequence in the 14-day post-transplant U3035Mt20-X3 chimeras was most similar to the donor U3020 line and had only retained a small proportion of the recipient mtDNA sequence.

mtDNA sequencing, indicating that the donor mitochondrial are retained in the recipient cell for at least two weeks, well beyond the standard doubling time of the U3035 GBM cells. Thus, the CPP-mediated mitochondrial transplantation from one GBM cell line to another appears to be achievable and durable within the context of our time course.

One feature that complicates the development of novel therapeutics in GBM research is that nearly all clinical trials are initially performed in the setting of recurrent disease after the delivery of standard of care first-line chemotherapy and external beam radiotherapy. Hence, we endeavored to explore the feasibility of using the CPP mitochondrial transplantation on GBM cells that were already radiation resistant. In generating U3035 cells exposed to serial radiotherapy doses, we confirmed that the CPP methodology can deliver donor mitochondria to radiation resistant cells, as would be the likely scenario in clinical investigation. Further studies will be needed to confirm if the ROS generated in response to subsequent radiation post-transplantation is similar to the radiation naïve cell studies.

The contribution of ROS as a tumorigenic versus therapeutic agent in setting of malignancy remains the subject of debate[33]. Whereas basal increases in ROS levels have been associated with neoplastic transformation, breaching the threshold past which ROS levels become toxic within tumor cells appears to be a viable therapeutic strategy as demonstrated by the numerous cancer treatments tasked with that same goal[34]. The fundamental question remaining to be answered pertains to the identification of the level at which ROS becomes lethal and if that level can be achieved using mitochondrial harvested from autologous tumor cells or autologous non-neoplastic tissue. As previously discussed, the stoichiometry of ROS production based on mitochondrial

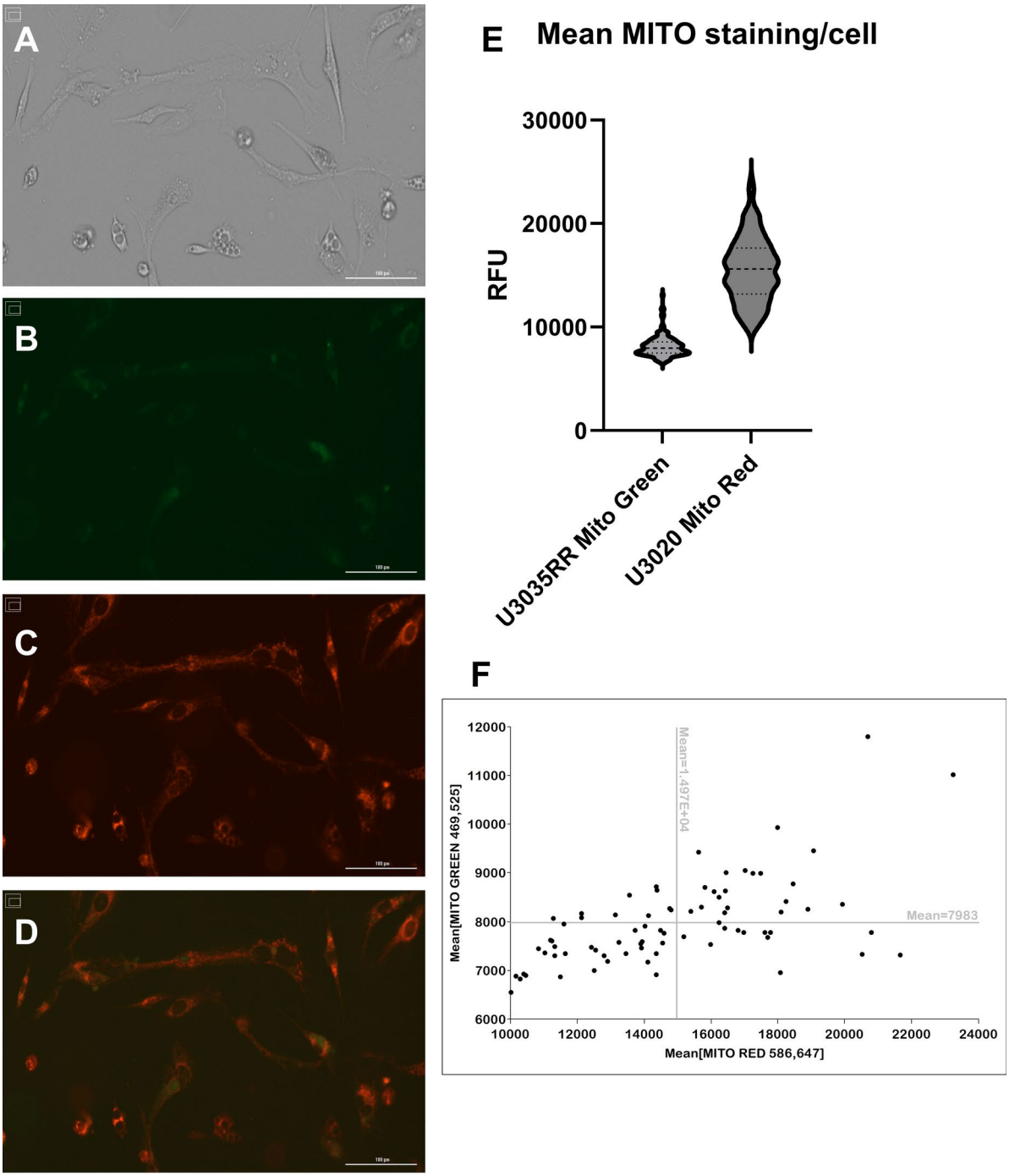

Fig. 7. Allogenic mitochondrial transplantation in radiation resistant GBM. Representative images of (**A**) Brightfield view (60X) of U3035 resistant to 12 Gy radiation (2 Gy × 6 fractions). (**B**) Native mitochondria in radiation resistant U3035 cells stained with 200 nM MitoTracker™ Green vital dye. (**C**) Transplanted mitochondria from U3020 cells stained with 200 nM MitoTracker™ Red vital dye. (**D**) Overlay image of the green and red fluorescent channels highlighting successful transfer. Images were obtained at post-transplant at 48 h at 60X magnification and using 469/525 nm; 586/647 nm filters. (**E**) Mean fluorescence image intensity was calculated for the native (MITO Green) and donor (MITO Red) channels for each cell (n = 141) and expressed on XY plot (**F**).

content in the present study mimics that of work completed in skeletal muscle[31]. From a practical perspective, one future area of study would be to examine the ability to successfully transplant mitochondria from skeletal muscle for determination of both ROS potential and durability. In the setting of recurrent GBM undergoing surgical resection, options for subsequent radiation delivery are very limited, usually using hypo-fractionated or radiosurgery techniques[35,36]. During surgery, local muscle is usually accessible as part of the standard

approaches. Harvesting a small amount of mitochondria-dense tissue with CPP preparation and injection into the presumption post-operative radiation target areas could afford a novel mechanism for increased lethal ROS generation.

Although we can conclude that our technique of mitochondrial transplantation into GBM cells was successful based on ROS generation and durability endpoints, there are limitations to the work. First, in the attempt to provide data on human-derived tumor cells, no in vivo rodent studies have been performed. While the majority of intracellular ROS generated in most cells is mitochondrial in origin, no confocal imaging was prepared to confirm the sub-cellular compartment localization. With respect to the EPR data, the availability of effective in vivo ROS probes is extremely limited. The ROS species, primarily hydroxyl radicals, are very short-lived and reduced quickly by antioxidant mechanisms, hence the need for spin-trap adduct use and quantification. Further characterization of the ROS generated beyond this would require analysis with additional spin-trap reagents, such as 5-(diethoxyphosphoryl)-5-methyl-1-pyrroline N-oxide (DEPMPO) for isolation of potential superoxide radicals as well as analysis of the decay rates as we have previously published for U3035 and U3020 cells[32].

Moreover, the proposed application of use in recurrent GBM, creates a further obstacle to create an immune-competent rodent model where data beyond the tolerability of surgery, radiation, and CPP use could be tested. Perhaps the greatest limitation of the current study lies in the lack of predictability of ROS lethality and the level to which intracellular ROS needs to reach to insure radiation-induced cell death. Further studies that incorporate the concurrent blockade of free-radical scavenger systems will be needed to optimize the techniques to achieve maximal results while minimizing radiation exposure.

Materials and methods

Cell lines

Three human mesenchymal subtype glioblastoma cell lines, U3035, U3020, and U3046 were obtained from the Human Glioblastoma Cell Culture (HGCC) Biobank at Uppsala University in Sweden. The cells were cultured in defined media (DMEM/F-12, EGF, FGF, N2, B27 supplements) with penicillin/streptomycin at 37 °C in 5% CO_2 according to recommended passaging parameters. Verification of cell line authenticity was performed via short tandem repeat (STR) analysis by ATCC in Manassas, VA, USA (supplemental data S1). A subset of U3020 and U3035 cells were cultured under hypoxic conditions (1% O_2) to assess native mitochondrial response to low oxygen levels using a C-Chamber Cytocentric® incubator sub-chamber (Biospherix, Parish, NY, USA).

Mitochondrial isolation and quantification

U3020 and U3035 cells were cultured in T75 flasks until 90% confluency was achieved. Cells were dissociated with Accutase® (Milipore Grp, Burlington, MA), pelleted via centrifugation, and resuspended in 1 mL mitochondrial isolation buffer. Cell counts were obtained using a Cellometer® Auto 2000 cell viability counter (Nexcelom™ Bioscience LLC, Lawrence, MA). Mitochondria were then isolated using a commercially available kit according to manufacturer's instructions (Biovision™, Milpitas, CA, USA). Briefly, reagent-based permeabilization was performed on whole cells to allow for mitochondrial extraction from the cytosolic space. Differential centrifugation first separated mitochondria from other cellular debris (600xg) and then isolated mitochondria from other biomolecular components of the cytosolic space (7000xg). Mitochondria were resuspended in a storage buffer and the total protein content of the mitochondria isolates were measured using a BioTek Take3 plate (Aligient, Santa Clara, CA) and optical density A280 quantification measurement.

Mitochondrial labeling and transplantation

Whole cells or mitochondria were labeled using Mitotracker™ (Thermo Fisher Scientific, Waltham, MA) vital dyes. Recipient cells (U3035; U3046) were seeded at a density of 5.0×10^5 cells/well of 6-well Corning CoStar geometry plate and allowed to adhere overnight. Media in each well was replaced with serum-free neural basal media containing 200 nM green MitoTracker™ dye and allowed to incubate at 37 °C 5.0% CO_2 for 30 min. Donor mitochondria (U3020; U3046) were isolated as described above and resuspended in neural basal media containing either 200 nM green (for post-transplant quantification) or red (proof-of-concept) MitoTracker™ dye for 30 min at 37 °C 5.0% CO_2. Dyed mitochondria were then incubated with a cell-penetrating peptide, Pep-1-Cysteamine (Pep-1) (suspended in 1X phosphate-buffered saline), at a ratio of 0.06 mg Pep-1/100 µg of mitochondrial protein in 400µL of PBS, as described by Chang et al.[37]. The mitochondria and Pep-1 were allowed to conjugate for 20 min at room temperature. Following the Pep-1 conjugation, either 400µL of 100 µg of mitochondrial protein (1X transplant) or 300 µg of mitochondrial protein (3X transplant) were added to recipient cells cultured in 6-well plates containing DMEM/F-12, EGF, FGF, N2, B27 supplements and 1% penicillin/streptomycin. Mitochondria were allowed to transplant over a period of 48 h after which fresh DMEM was replaced. Images of successful transplants were taken at 48 h.on BioTek Cytation 5 cell imaging system (Aligent, Santa Clara, CA). Resulting mitochondrial chimeras were continued in culture for 14 days to determine transplant durability. Fluorescent intensity of 1X 3X chimeras were quantified using BioTek Gen5 software (Aligent, Santa Clara, CA). Individual cells were auto-segmented and analyzed for mean intensities of each channel (469/525 nm; 586/647 nm) with brightfield microscopy image mask controls. Mean intensities were expressed as composite violin graphs and XY scatter plots with data points for each individual cell (GraphPad Prism 10.4.0). Western blotting was performed on the U3035 native cells and autologous 1X and 3X transplants. RIPA extraction was completed on $1X10^7$ cells and protein determination performed by Pierce BCA (ThermoFisher Scientific, Waltham, MA). 10 µg and 5 µg aliquots of each sample were resolved via Novex™ Tris–Glycine 4–12% gels and transferred with nitrocellulose for blotting against Cytochrome C (7H8; Santa Cruz Biotechnology, Dallas, TX), 1:200 with HRP-conjugated mouse IgG Fc binding protein (1:1000). Chemiluminescence was developed with the SuperSignal™ West Dura Extended Duration Substrate and images captured on the Amersham ImageQuant 800 (Cytiva Life Sciences, Marlborough, MA).

Mitochondrial DNA extraction

Mitochondrial DNA was extracted directly from freshly isolated mitochondria following the protocols outlined by Abcam (Cambridge, United Kingdom). Briefly, an enzymatic mixture (proteinase K and RNAse) was allowed to incubate with the mitochondria for 30 min at 55 °C. Mitochondrial samples were then mixed with an alkaline lysis buffer (containing NaOH), allowed to incubate on ice for 5 min. An acidic neutralization buffer (containing glacial acetic acid) was then added to the sample tubes. Mitochondrial DNA samples were then separated via centrifugation and the supernatants were added to DNA trapping spin columns. This supernatant was spun through the columns and washed twice using a wash buffer containing 75% ethanol. DNA samples were then eluted with a Tris–HCl/EDTA buffer at room temperature for 2 min. Samples were recovered from columns using centrifugation and DNA quality and quantity were measured using A_{260} and $A_{260/280}$ determinations.

Mitochondria DNA sequencing and analyses

Mitochondrial DNA concentrations were quantified using a Qubit 4 Fluorometer (ThermoFisher Scientific, Waltham, MA). The SparQ DNA Fragment and Library Prep kit was used to build the mitochondrial DNA libraries using 1–4 ng of template according to protocol. The completed libraries were quantified using the Qubit and run on an Agilent Bioanalyzer with the High Sensitivity DNA chip to determine the average size of each library. The libraries were pooled together, at an equal molar ratio, and run on a Miseq with an Illumina V2 300 cycle (PE150bp) reagent kit.

Adapter sequences were trimmed from all FASTQ files using Atria (version 4.0.3; RRID:SCR_021313). Successful removal of adapter sequences was confirmed using FastQC (version 0.12.1; RRID:SCR_014583). NOVOPlasty (version 4.3.5; RRID:SCR_017335) was then used for de novo assembly of the mitochondrial genome using adapter trimmed deep sequencing reads from the U3020 parental line with the following input parameters: genome size constraint 12–22 kilobases, K-mer of 33, and DNA sequence for MT-ATP8 (gene ID: 4509) from GRCh38.p14 as the seed. Single nucleotide polymorphisms (SNPs) in the U3035 parental line relative to the constructed U3020 mitochondrial genome assembly were detected using the heteroplasmy function of NOVOPlasty. A total of 39 such SNPs were detected at homoplasmic allele frequencies (≥0.99) in the U3035 parental line. The U3035 14-day U3035Mt20-3X chimera was then compared to the same U3020 mitochondrial genome assembly. A total of 37 SNPs were detected at heteroplasmic allele frequencies (0.01–0.99) with 32 of the 37-sharing identity with homoplasmic SNPs identified in the U3035 parental line. Percent similarity was then determined by averaging the variant allele frequencies for the 32 shared SNPs. All data were graphically presented using Circos circular ideogram visualization[38].

Cell irradiation and reactive oxygen species measurements

All cell lines receiving radiation for ROS evaluation (U3035, U3020, U3035-U3020 1X; U3035-U3020 3X) were exposed to 8 Gy of ionizing radiation (220 kV, 13 mA) using a XenX radiation platform (Xstrahl; Suwanee, GA) to determine if there were differential generation of reactive oxygen species (ROS) between the cell lines. Previous studies using U3035 and U3020 cells had established the dose of 8 Gy as effective with doses ranging from 4 to 20 Gy[32]. 5.0×10^5 cells were suspended in 200 mM DMPO, irradiated, and subsequently probed using electron paramagnetic resonance (EPR) via and ELEXSYSII spectrometer (Bruker; Billerica, MA) for quantification of hydroxyl radical production. All lines were also probed for ROS generation, primarily hydroxyl and superoxide species, using CellROX™ red dyes (ThermoFisher Scientific; Waltham, MA). Briefly, cells were given 5 nM of the CellROX™ dye in their native 6-well plate and DMEM immediately prior to exposure to 8 Gy of ionizing radiation (220 kV, 13 mA). Cell lines were assayed again 24 h following irradiation. Non-irradiated, CellROX™ treated cells and irradiated cells with no CellROX™ reagent were used as positive and negative controls, respectively. Samples were allowed to incubate at 37 °C 5.0% CO_2 for 30 min. Images were acquired using the BioTek Cytation 5 Cell Imaging Multimode Reader. A subset of U3035 cells were irradiated at 2 Gy (220 kV, 13 mA) every other day, for 12 days, to generate a 12 Gy radioresistant cell line to determine if mitochondrial transplantation was feasible in cells which are not radiation naïve. These radiation resistant U3035 cells were used to generate U3035RR-U3020 1X chimera.

Data availability

The datasets generated and analyzed during the current study are available in the NCBI BioProject repository under accession number PRJNA1134145 or individual sequences at NCBI Sequence Read Archive (SRA) under accession numbers SRX25532763, SRX25532762, and SRX25532761.

Received: 1 August 2024; Accepted: 19 February 2025
Published online: 04 March 2025

References

1. Stupp, R. et al. Effect of tumor-treating fields plus maintenance temozolomide vs maintenance temozolomide alone on survival in patients with glioblastoma: A randomized clinical trial. *JAMA* **318**(23), 2306–2316 (2017).
2. Stupp, R. et al. Radiotherapy plus concomitant and adjuvant temozolomide for glioblastoma. *N. Engl. J. Med.* **352**(10), 987–996 (2005).
3. McBain, C. et al. Treatment options for progression or recurrence of glioblastoma: a network meta-analysis. *Cochrane Database Syst. Rev.* **5**(1), CD013579 (2021).
4. Goenka, A. et al. The many facets of therapy resistance and tumor recurrence in glioblastoma. *Cells* **10**(3) (2021).
5. Minniti, G. et al. Current status and recent advances in reirradiation of glioblastoma. *Radiat. Oncol.* **16**(1), 36 (2021).
6. Sia, J. et al. Molecular mechanisms of radiation-induced cancer cell death: A primer. *Front. Cell Dev. Biol.* **8**, 41 (2020).
7. Kim, W. et al. Cellular stress responses in radiotherapy. *Cells* **8**(9) (2019).

8. Zheng, Z. et al. Mechanisms and applications of radiation-induced oxidative stress in regulating cancer immunotherapy. *Front. Immunol.* **14**, 1247268 (2023).
9. Napolitano, G., Fasciolo, G., & Venditti, P. Mitochondrial management of reactive oxygen species. *Antioxidants (Basel)* **10**(11) (2021).
10. Murphy, M. P. How mitochondria produce reactive oxygen species. *Biochem. J.* **417**(1), 1–13 (2009).
11. Meng, Q. et al. Possible relationship between mitochondrial changes and oxidative stress under low dose-rate irradiation. *Redox. Rep.* **26**(1), 160–169 (2021).
12. Kawamura, K., Qi, F., & Kobayashi, J. Potential relationship between the biological effects of low-dose irradiation and mitochondrial ROS production. *J. Radiat. Res.* **59**(suppl_2), ii91–ii97 (2018).
13. Vringer, E. & Tait, S. W. G. Mitochondria and cell death-associated inflammation. *Cell Death Differ.* **30**(2), 304–312 (2023).
14. Lo Cascio, C. et al. Quisinostat is a brain-penetrant radiosensitizer in glioblastoma. *JCI Insight* **8**(22) (2023).
15. Ali, M. Y. et al. Radioresistance in glioblastoma and the development of radiosensitizers. *Cancers (Basel)* **12**(9) (2020).
16. Nabors, L. B. et al. Central nervous system cancers, Version 3.2020, NCCN Clinical Practice Guidelines in Oncology. *J. Natl. Compr. Canc. Netw.* **18**(11), 1537–1570 (2020).
17. Vogelbaum, M. A. et al. Treatment for brain metastases: ASCO-SNO-ASTRO guideline. *J. Clin. Oncol.* **40**(5), 492–516 (2022).
18. Zhang, T. G. & Miao, C. Y. Mitochondrial transplantation as a promising therapy for mitochondrial diseases. *Acta Pharm. Sin. B* **13**(3), 1028–1035 (2023).
19. Damato, M. et al. Mitochondrial transplantation in mitochondrial medicine: Current challenges and future perspectives. *Int. J. Mol. Sci.* **24**(3), 1 (2023).
20. Chang, J. C. et al. Treatment of human cells derived from MERRF syndrome by peptide-mediated mitochondrial delivery. *Cytotherapy* **15**(12), 1580–1596 (2013).
21. Mellinghoff, I. K. et al. Vorasidenib in IDH1- or IDH2-mutant low-grade glioma. *N. Engl. J. Med.* **389**(7), 589–601 (2023).
22. Louis, D. N. et al. The 2021 WHO classification of tumors of the central nervous system: A summary. *Neuro Oncol.* **23**(8), 1231–1251 (2021).
23. Chien, C. H. et al. Enrichment of superoxide dismutase 2 in glioblastoma confers to acquisition of temozolomide resistance that is associated with tumor-initiating cell subsets. *J. Biomed. Sci.* **26**(1), 77 (2019).
24. Li, H. Y. et al. Mitochondrial mechanisms in Temozolomide resistance: Unraveling the complex interplay and therapeutic strategies in glioblastoma. *Mitochondrion* **75**, 101836 (2024).
25. Huang, H. et al. Suppression of mitochondrial ROS by prohibitin drives glioblastoma progression and therapeutic resistance. *Nat. Commun.* **12**(1), 3720 (2021).
26. Pinto, G. et al. Patient-derived glioblastoma stem cells transfer mitochondria through tunneling nanotubes in tumor organoids. *Biochem. J.* **478**(1), 21–39 (2021).
27. Valdebenito, S. et al. Tunneling nanotubes, TNT, communicate glioblastoma with surrounding non-tumor astrocytes to adapt them to hypoxic and metabolic tumor conditions. *Sci. Rep.* **11**(1), 14556 (2021).
28. Tashima, T. Intelligent substance delivery into cells using cell-penetrating peptides. *Bioorg. Med. Chem. Lett.* **27**(2), 121–130 (2017).
29. Guan, J. et al. Short peptide-mediated brain-targeted drug delivery with enhanced immunocompatibility. *Mol. Pharm.* **16**(2), 907–913 (2019).
30. Zong, T. et al. Enhanced glioma targeting and penetration by dual-targeting liposome co-modified with T7 and TAT. *J. Pharm. Sci.* **103**(12), 3891–3901 (2014).
31. Ljubicic, V. & Hood, D. A. Kinase-specific responsiveness to incremental contractile activity in skeletal muscle with low and high mitochondrial content. *Am. J. Physiol. Endocrinol. Metab.* **295**(1), E195-204 (2008).
32. Cifarelli, C. P., Jacques, A. & Bobko, A. Heterogeneity of radiation response in mesenchymal subtype glioblastoma: Molecular profiling and reactive oxygen species generation. *J. Neurooncol.* **152**(2), 245–255 (2021).
33. Zou, Z. et al. Induction of reactive oxygen species: An emerging approach for cancer therapy. *Apoptosis* **22**(11), 1321–1335 (2017).
34. Galadari, S. et al. Reactive oxygen species and cancer paradox: To promote or to suppress?. *Free Radic. Biol. Med.* **104**, 144–164 (2017).
35. Kazmi, F. et al. Re-irradiation for recurrent glioblastoma (GBM): A systematic review and meta-analysis. *J. Neurooncol.* **142**(1), 79–90 (2019).
36. Bunevicius, A. et al. Stereotactic radiosurgery for IDH wild type glioblastoma: An international, multicenter study. *J. Neurooncol.* **155**(3), 343–351 (2021).
37. Chang, J. C. et al. Peptide-mediated delivery of donor mitochondria improves mitochondrial function and cell viability in human cybrid cells with the MELAS A3243G mutation. *Sci. Rep.* **7**(1), 10710 (2017).
38. Krzywinski, M. et al. Circos: An information aesthetic for comparative genomics. *Genome Res.* **19**(9), 1639–1645 (2009).

Author contributions

CPC and KLM made substantial contributions to the design of the work, data acquisition, analysis, and drafting of the manuscript. MV, VVK and AM contributed to data acquisition and manuscript preparation. All authors reviewed final draft prior to submission.

Declarations

Competing interests

CPC has been funded by NIGMS P20GM121322, NIH U54GM104942. He has received unrelated speaking honoraria from Carl Zeiss Meditech AG. KLM, AM, VVK and MV declare no potential conflict of interest.

Additional information

Supplementary Information The online version contains supplementary material available at https://doi.org/10.1038/s41598-025-91331-2.

Correspondence and requests for materials should be addressed to C.P.C.